Nano Energy 43 (2018) 228–235

Contents lists available at ScienceDirect

Nano Energy

journal homepage: www.elsevier.com/locate/nanoen

Full paper

Improved amorphous silicon passivation layer for heterojunction solar cells with post-deposition plasma treatment

Alex Neumüller[a,*], Oleg Sergeev[a], Stephan J. Heise[b], Segei Bereznev[c], Olga Volobujeva[c], Jose Fabio Lopez Salas[b], Martin Vehse[a], Carsten Agert[a]

[a] DLR-Institut für Vernetzte Energiesysteme, Carl-von-Ossietzky-Straße 15, 26129 Oldenburg, Germany
[b] Laboratory for Chalcogenide Photovoltaics, Department of Energy and Semiconductor Research, Institute of Physics, University of Oldenburg, 26111 Oldenburg, Germany
[c] Department of Materials Science, Tallinn University of Technology, Ehitajate tee 5, Tallinn 19086, Estonia

ARTICLE INFO

Keywords:
a-Si
PECVD
Interface
SHJ
Argon
Hydrogen

ABSTRACT

In numerous silicon semiconductor devices, an important task is to suppress charge carrier recombination at surface dangling bonds. In solar cell business, silicon heterojunction with intrinsic thin film (SHJ) solar cells is one of the major research topics to investigate and optimize such interface defect states. The aim of this work is to further optimize SHJ solar cells by post-deposition argon plasma treatment (APT) and to demonstrate the origin of material improvement compared to hydrogen plasma treatment (HPT). We analyze the influence of post-deposition APT and HPT on the surface of 10 nm thick intrinsic hydrogenated amorphous silicon (i-a-Si:H) layers and show the influence of this advanced post-deposition passivation technique on SHJ solar cells. For the first time a detailed study is presented here which could be also applied to several other techniques.

The results demonstrate that our approach of post-deposition plasma treatment distinctly optimizes the i-a-Si:H/c-Si interface by restructuring the i-a-Si:H layer itself. It is discussed that argon or hydrogen plasma treatment steps applied to a-Si:H/c-Si structures can lead to an improved chemical passivation. Other than expected, APT shows beneficial effects by increasing significantly the minority carrier lifetime, material compactness and the splitting of quasi-Fermi levels compared to HPT. We also discuss the origin of enhanced interface properties after post-deposition APT and fabricated $2 \times 2\ cm^2$ lab cells with an outstanding increase in open-circuit voltage compared to reference cells without APT, to a maximum of 720.5 mV.

1. Introduction

Interfaces play a crucial role in numerous semiconductor devices. Several attempts to suppress charge carrier recombination at surface dangling bonds of crystalline silicon (passivation), such as silicon oxide [1–3], silicon nitride [4–6], silicon carbide [7] and aluminum oxide [8,9] have been successfully applied to silicon heterojunction (SHJ) solar cells. Alternatively, intrinsic hydrogenated amorphous silicon (i-a-Si:H) can be used [10]. High-quality i-a-Si:H layers have been developed to saturate dangling bonds [11] in SHJ solar cells. This concept of silicon heterojunction with intrinsic thin film solar cells (SHJ-SC) has led to a world record efficiency of 25.6% on a total cell area of 143.7 cm^2 [12].

Despite the high conversion efficiencies achieved with SHJ-SC's, further improvements can be achieved by understanding the influences to a thin i-a-Si:H layer, e.g. due to post-deposition plasma treatment.

So far HPT has been introduced as state-of-the-art interface plasma treatment method by several research groups. Mews et al. demonstrated that e.g. hydrogen can prevent i-a-Si:H layers from epitaxial growth, leading to deposition conditions close to the amorphous to microcrystalline transition that improves the passivation quality of the thin i-a-Si:H layers [13]. Zhang et al. reported recently that using hydrogen plasma treatment before or after i-a-Si:H depositions leads to superior minority carrier lifetimes compared to reference substrates without hydrogen plasma treatment [14]. Descoeudres et al. have shown that several hydrogen plasma treatment steps during the i-a-Si:H deposition can be beneficial to increase the minority carrier lifetime [15]. Smets et al. deduced from their experiments that argon ion bombardment is advantageous during the i-a-Si:H growing processes when several plasma conditions are fulfilled [16]. In some studies, the ion bombardment has been found not to be detrimental to the plasma-enhanced chemical vapor deposition (PECVD) growth of high-quality a-Si:H films

* Corresponding author.
E-mail addresses: alex.neumueller@uni-oldenburg.de (A. Neumüller), oleg.sergeev@dlr.de (O. Sergeev), stephan.heise@uni-oldenburg.de (S.J. Heise), sergei.bereznev@ttu.ee (S. Bereznev), olga.volobujeva@ttu.ee (O. Volobujeva), jose.fabio.lopez.salas@uni-oldenburg.de (J.F.L. Salas), martin.vehse@dlr.de (M. Vehse), carsten.agert@dlr.de (C. Agert).

https://doi.org/10.1016/j.nanoen.2017.11.053
Received 17 September 2017; Received in revised form 22 November 2017; Accepted 23 November 2017
Available online 24 November 2017

[17].

Despite the fact that various performance limiting factors concerning interface quality have been recently addressed, post-deposition plasma treatments are not widely discussed in the literature. In particular, the effect of post-deposition plasma treatment and the accompanying ion bombardment should be further investigated as it could be beneficial for silicon heterojunction solar cells [18]. Addressing interface plasma treatment methods could gain a deeper understanding of the interfaces especially the heterointerface between i-a-Si:H/c-Si for the usage in SHJ solar cells.

In the present study, we extend previous HPT studies on thin i-a-Si:H layers to unique argon treated interfaces and compare both methods with each other on a few nanometer thin i-a-Si:H layers. We analyze the differences between both methods by showing the influence on the material properties of thin i-a-Si:H layers using spectroscopic ellipsometry and infrared measurements as well as demonstrating the overall positive effect applying effective minority carrier lifetime measurements. Further, we carry out photoluminescence (PL) and surface photovoltage (SPV) experiments. Finally, we apply for the first time argon plasma treatment at the interface in silicon heterojunction solar cells. To fully cover all investigations we compare the effect of APT and HPT on SHJ solar cells.

2. Methods

2.1. Depositions and samples

Textured (111) n-type Czochralski (CZ) silicon (c-Si) wafers with an average resistivity of 5 Ω cm and a thickness of 130 µm were used in general to fabricate the test layer structure as depicted in Fig. 1a. As several measurements required flat surfaces, double side polished (100) float zone (FZ) n-doped silicon wafers were used in addition. Prior to deposition, the substrates were immersed into a 1% HF solution for 3 min. This step is followed by symmetrically 13.56 MHz PECVD deposited i-a-Si:H layers. After deposition, the substrates were exposed to an argon or hydrogen plasma which led to ion bombardment on the surface [15,16,19].

In this study, we demonstrate the effect of APT or HPT for two sets of samples, labeled *LP* for low-power and *HP* for high-power, as summarized in Table 1. In series *LP* the deposition power density (RF-P) was set to 19 mW/cm^2 and the hydrogen dilution, $R = \phi(H_2)/\phi(SiH_4)$, was varied from 0 to 2.5. The second series was deposited at a power density of 38 mW/cm^2 and same values for R. In order to guarantee the same layer thickness between the series the deposition times were adjusted according to the growth rate.

The heater temperature, deposition pressure and the distance between the electrodes in the PECVD chamber were kept similar for all deposited i-a-Si:H layers at 200 °C, 1 mbar and 20 mm, respectively.

Table 1
Deposition parameters of series *LP* and series *HP* samples. Columns three and four show the respective plasma parameters of APT and HPT.

	Series *LP*	Series *HP*	APT	HPT
SiH_4 [sccm]	40	40	–	–
H_2 [sccm]	0–100	0–100	–	200
Ar [sccm]	–	–	200	–
RF-P [mW/cm^2]	19	38	19	19
p [mbar]	1	1	1	1
$d_{elec.}$ [mm]	20	20	25	25
T_{heater} [°C]	200	200	200	200
t_{depo} [s]	29–60	18–45	60	120

APT and HPT treatment parameters are summarized in Table 1. During all plasma treatment (PT) depositions the power density, the deposition pressure, and the electrode distance were kept constant at 200 °C, 1 mbar and 25 mm, respectively. Argon or hydrogen gas flow rate was set to $\phi(Ar, H_2) = 200$ sccm. Finally, the symmetric heterostructure of PT/i-a-Si:H (10 nm)/c-Si/i-a-Si:H (10 nm)/PT was fabricated and later annealed at 190 °C for 90 min to reduce the effect of dangling bonds caused by inhomogeneous microstructure [20].

2.2. Experimental

All experiments in the framework of this study were conducted using contactless measurements techniques to determine the absorber, interface and passivation quality without destructive influences on the interfaces.

Optical measurements were made by spectroscopic ellipsometry (Sentech SE850) and a Fourier transformed infrared (FTIR) PerkinElmer Spectrum 400 tool on double-side polished FZ c-Si wafers. For the accurate determination of the simulated nk data, reflection spectra and ellipsometry measurements (Ψ and Δ data) of the layers were carried out. In contrast to previous publications we chose the so-called O'Leary–Johnson–Lim (OJL) model [21] instead of the Tauc–Lorentz model [22] to calculate the imaginary part of the dielectric function and to extract data of the optical transition strength (just *strength* hereafter) from that, which is correlated to the material's compactness. Therefore, high-quality materials are characterized by high or increasing optical transition strength values. The data were evaluated with a commercial software (SCOUT/CODE, W. Theiss Hard- and Software).

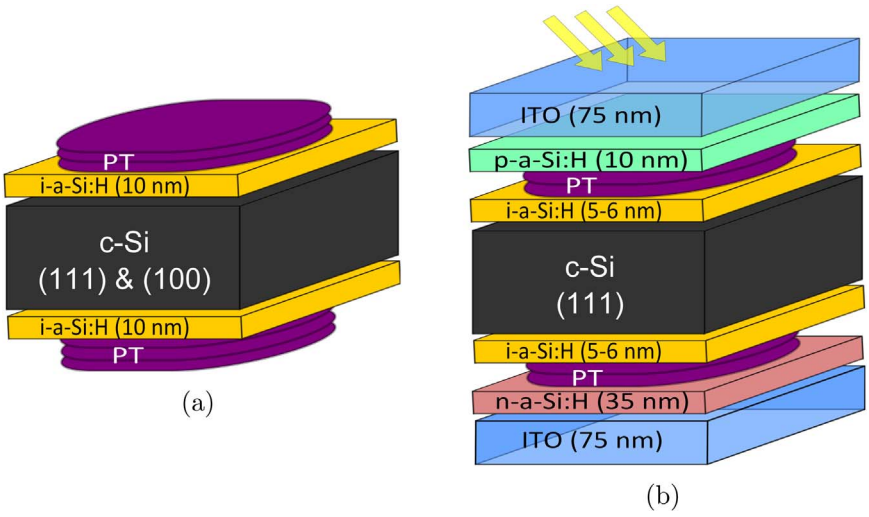

Fig. 1. (a) Experimental single layer stack. (b) Layer stack of SHJ solar cells fully fabricated in PECVD cluster tool.

The infrared spectrum was deconvoluted using two Gaussian modes around $\nu_1 = 2000\ \mathrm{cm}^{-1}$ and $\nu_2 = 2100\ \mathrm{cm}^{-1}$ to calculate the microstructure factor (*ms*). If two or more hydrogen atoms (polyhydride bonds) are bonded to a silicon atom at a void surface, their stretching vibration modes form at higher wavenumber around $\nu = 2100\ \mathrm{cm}^{-1}$ [23,24].

The effective minority carrier lifetime (τ_{eff}) was determined using Sinton instruments WCT-120 equipment at a carrier injection level of $\Delta n = 1{\cdot}10^{15}\ \mathrm{cm}^{-3}$ and 1 sun. Additionally the effective surface recombination velocity (S_{eff}) was determined for some samples following the equation:

$$S_{eff} = \left(\frac{1}{\tau_{eff}} - \frac{1}{\tau_b}\right)\cdot\frac{W}{2}. \quad (1)$$

Here, τ_b is the bulk lifetime, set to $\tau_b = 1$ ms according to producer standards, and W is the wafer thickness (W = 130 μm). We used Eq. (1) to incorporate this into the model suggested by Olibet et al. [25]. They introduced a two-dimensional model to calculate the i-a-Si:H/c-Si interface defect state density N_s [cm^{-2}] based on recombination via amphoteric defects, i.e. silicon dangling bonds. It should be noted that the values obtained are not absolute as they strongly depend on some factors which have been taken from different references [25–27]. However, they can be used for a relative comparison.

PL spectra have been measured in the photon energy range of $0.95 - 1.38$ eV($900 - 1300$ nm), at room temperature (295 K) and with a constant excitation laser intensity of approximately 932 mWcm^{-2}. If the absorption (A) is assumed to be A(E) = 1 for energies higher than the optical bandgap, $E > E_g$, the temperature T and the splitting of the quasi-Fermi levels (μ) may be extracted from the PL spectra by fitting Planck's generalized equation after Boltzmann approximation

$$Y_{PL} = \frac{\Omega}{4\pi^3\hbar^3c^2}\cdot\exp\left(-\frac{(E-\mu)}{k_B T}\right)\cdot E^2 \quad (2)$$

to the high-energy wing of the spectrum [28]. In Eq. (2), Y_{PL} is the detected photon flux in a solid angle Ω. In our case the setup was not calibrated for absolute photon fluxes, therefore only relative differences of μ between samples measured under the same conditions could be derived.

Kelvin probe measurements were performed under illumination (surface photovoltage, SPV) and non-illumination by scanning Kelvin probe system (SKP5050) equipped with 2 mm gold-covered vibrating tip and under pulsed laser irradiation (670 nm, 20 $\mathrm{mW/cm}^2$ intensity) [29]. The resulting change in the potential is recorded as ΔSPV.

In addition to the single layer characterization we fabricated several SHJ solar cells and measured the pseudo fill factor (pFF), the pseudo open-circuit voltage (pV_{oc}) and the pseudo solar conversion efficiency (pη) using a Suns − V_{oc} set-up (Sinton WCT 120). In Fig. 1b the deposited layer stack is depicted. We used a 5–6 nm thick i-a-Si:H layer deposited at a power density of 38 $\mathrm{mW/cm}^2$ with a hydrogen dilution of R = 2.5. The depositions were performed on the same textured CZ silicon wafers, 156 cm^2 and 130 μm thick. After i-a-Si:H layer deposition either APT or HPT was applied from both sides to the layer prior to the subsequent deposition of the n- and p-layers. 75 nm thick ITO electrodes were deposited on both sides as front and back contacts.

All measurement errors were determined by means of multiple measurements, either in different points or on different samples. Error bars of individual measurements were determined from the standard deviation. Otherwise, an instrumental error of 5% was assumed.

3. Results and discussion

In this section, the innovative argon plasma treatment technique is compared to hydrogen plasma treatment. The influence on material properties such as compactness, void structure, chemical passivation quality and radiative recombination were studied to show the effects on the interface upon plasma treatment. Finally, we demonstrate the effect of APT and HPT to SHJ solar cells illuminated from the emitter side (p-layer) and compare this results with SHJ solar cells without interface plasma treatment.

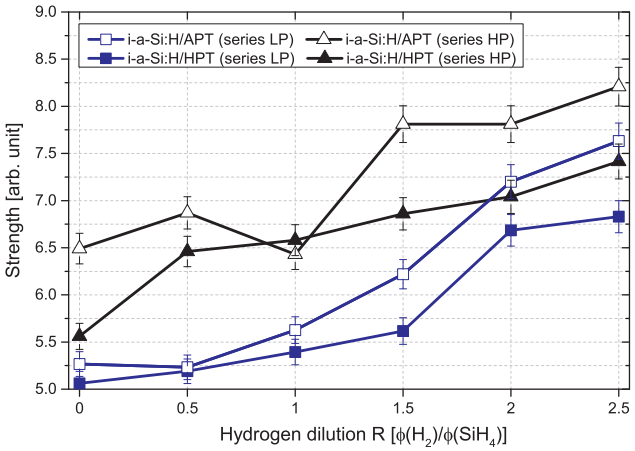

Fig. 2. Simulated strength values of series *LP*, series *HP* (blue and black lines) and a reproduced *reference* i-a-Si:H/APT samples are depicted.

3.1. Structural film characterization

From ellipsometry measurements extracted strength evolution of different i-a-Si:H layers (series *LP* & *HP*) deposited on (100) c-Si wafers are depicted in Fig. 2. The blue curves represent i-a-Si:H layers deposited at 19 $\mathrm{mW/cm}^2$ (series *LP*) while the black lines represent the i-a-Si:H layers deposited at 38 $\mathrm{mW/cm}^2$ (series *HP*). Argon treated samples are displayed by open symbols while hydrogen treated samples are represented by full symbols. Unless otherwise stated, this nomenclature is used for all illustrations.

As the hydrogen dilution increases from R = 0 to R = 2.5, an increase in the strength is clearly visible for both series. Furthermore, a significant increase in strength after APT, compared with HPT can be seen. Strength values obtained at R = 0 from series *LP* samples show that the strength after APT and HPT is 5.3 and 5.0, respectively. With increasing R, the strength increases almost linearly up to 7.6 and 6.6 after APT and HPT, respectively. The same trend but with higher initial strength (at R = 0) can also be seen for series *HP*. After APT the strength increases from 6.5 to 8.2 at R = 0 and R = 2.5, respectively. With HPT samples it is found that the strength is comparatively smaller, 5.6 for R = 0 and 7.4 for R = 2.5, respectively. It can be summarized that independently of the series, post-deposition APT more effectively restructures the silicon network due to argon ion bombardment and the cracking of weak Si bonds compared to HPT. According to Mews et al. hydrogen diffusion to the heterointerface and subsequent dangling bond passivation takes place during post-deposition HPT but due to the same process, the material compactness is reduced [13]. In our case, it seems that HPT influences the i-a-Si:H passivation layer similarly, explaining the relatively lower strength values.

To determine the relationship between argon ion bombardment and i-a-Si:H layer properties Smets et al. report that argon ion interaction during the i-a-Si:H layer deposition is responsible for film property modifications. They demonstrate that i-a-Si:H layer growth process diluted with argon is characterized by a reduction in the nanosized void density, a reduction in defect density, and an improvement of the photoresponse [16]. To verify the changes seen in this work and to correlate them with the results found by Smets et al. i-a-Si:H layers diluted with argon were prepared (R = 2.5, RF − P = 38 $\mathrm{mW/cm}^2$, ϕ(Ar = 200 sccm). From this experiment, the average value for the strength of 8.4 was obtained. Therefore, the values for i-a-Si:H layers diluted with argon and post-deposition argon treated i-a-Si:H layers

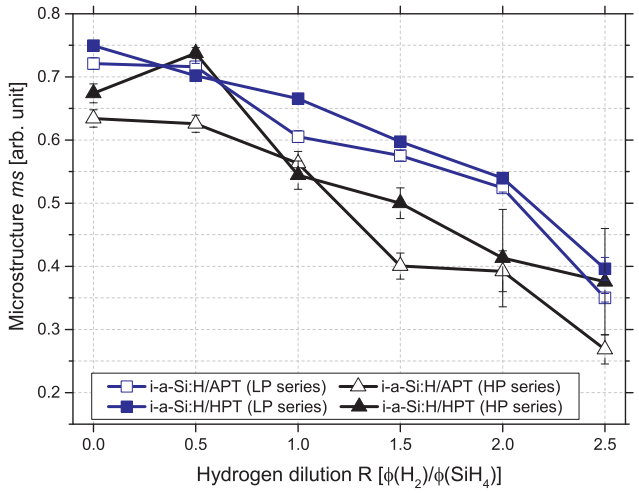

Fig. 3. Microstructure factor *ms* results of series *LP* (blue line) and series *HP* (black line) obtained from FTIR measurements.

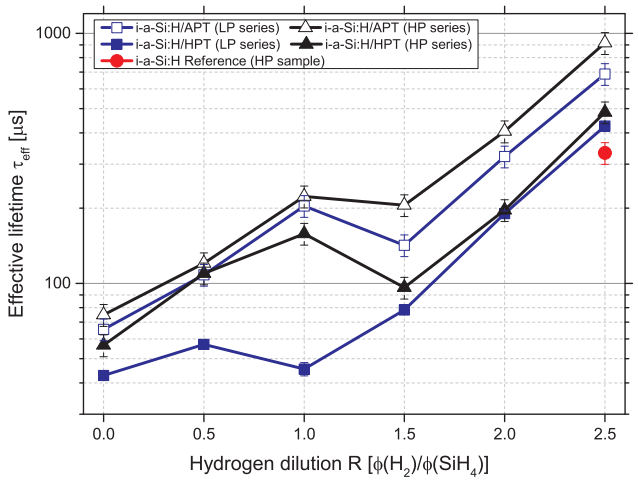

Fig. 4. Correlation of effective lifetime (τ_{eff}) measurements with deposition power density (RF-P) of single i-a-Si:H layers (series *LP* and series *HP*) and post-deposition plasma treatment (black and blue points). A reference i-a-Si:H sample without post-deposition PT is marked with a red point.

have similar strength values of 8.4 and 8.2, respectively. We conclude from these values, that post-deposition plasma treatment on thin i-a-Si:H layers (at least for thicknesses of up to 10 nm) have a similar effect as i-a-Si:H layers diluted with argon during the deposition.

Several publications show that the microstructure factor correlates with the defect density [30–32]. Therefore, the *ms* factor is an ideal indicator to get a deeper understanding of general a-Si:H material properties after PT. In Fig. 3 the *ms* of series *LP*, series *HP* and two different PT methods are depicted. The figure shows that the *ms* after APT, in the case of series *LP* and series *HP*, is smaller than after HPT. Analyzing series *LP* we see that at hydrogen dilution R = 2.5 after APT and HPT the *ms* factor is 0.35 and 0.4, respectively. For R = 0 the *ms* factor is increasing almost linearly to 0.72 and 0.75 after APT and HPT, respectively. In the case of series *HP*, the *ms* factor decreases further to 0.27 and 0.38 after APT and HPT, respectively. The resulting *ms* factor at R = 0 of series *HP* shows the same trend as series *LP* samples with *ms* factor values of 0.63 and 0.67 after APT and HPT, respectively. When comparing Figs. 2 and 3, the reciprocal behavior of strength and the *ms* factor is obvious. Especially at R = 1 the correlation of series *HP* results is visible as the calculation of the *ms* factor shows the same trend breaking jump, which can be considered as an outlier.

Toyoshima et al. reported that hydrogen is found to be incorporated into the films mainly by monohydride configuration during argon diluted CVD i-a-Si:H layer deposition due to improved structural relaxation [33]. Our results show that APT has a similar effect as argon diluted i-a-Si:H depositions that were demonstrated by Toyoshima et al. [33]. We found that silicon rearrangement is responsible for various improvements to material properties via enhanced surface migration, thus neutralizing and releasing material stress. In conclusion, it can be stated that APT samples are more compact due to lower microstructure factor and higher strength for both sample types.

In our previous work we have studied the polyhydride modes (dihydride and trihydride) [34,35] and the isolated monohydride modes [24] of silicon hydrogen chemical bonds by calculating the hydrogen content of a given mode [36]. The obtained results are indicating that the interface or the i-a-Si:H bulk structure changes after argon plasma treatment is highly dependent on the i-a-Si:H layer thickness and thus on the penetration depth of the argon or hydrogen ions.

In case of the highest dilution ratio, R = 2.5, the microstructure is decreasing after APT compared to HPT due to a change of the silicon–hydrogen vibrational modes. More precisely, APT does not change the hydrogen concentration while reducing the silicon–polyhybride bonds which are considered advantageous for high-quality i-a-Si:H layers. Although HPT is used as state-of-the-art plasma treatment to reduce dangling bonds at the interface in silicon heterojunction it increases the amount of clustered monohydrides and polyhydrides and decreases the number of isolated monohydride bonds.

3.2. Passivation and interface characterization

So far, our analysis methods were based on optical measurements for characterization of structural i-a-Si:H material changes upon argon or hydrogen plasma treatment. In the following section we focus on the recombination behavior of minority carriers in the bulk and at the interfaces of symmetrically passivated c-Si(n) wafers, studying the chemical passivation of post-deposition plasma treated i-a-Si:H layers.

The effective lifetime (τ_{eff}) results of series *LP* and series *HP* are summarized in Fig. 4. Both sample series show an increasing τ_{eff} with R and τ_{eff} for APT compared to HPT. In addition we add the lifetime result of an i-a-Si:H reference sample without post-deposition PT (red colored full circle) deposited at 38 mW/cm^2 and R = 2.5. This reference sample had the lowest effective lifetime (τ_{eff} = 333 µs) of all. From Fig. 4 we can see that τ_{eff} differs significantly between APT and HPT samples at higher values of R. After HPT the effective lifetime τ_{eff} of series *LP* increases from (42 ± 5) µs to (426 ± 9) µs with increasing hydrogen dilution. The second series shows a similar increase after HPT from (56 ± 5) µs to (483 ± 48) µs. Post-deposition APT exposed series *LP* and series *HP* samples show effective lifetimes of (65 ± 7)µs and (78 ± 9) µs, respectively, deposited at the lowest hydrogen dilution (R = 0). These values already show significant improvements in the effective lifetime compared to HPT. However, the lifetime further increases with increasing hydrogen dilution to the respective maximum values of (688 ± 69) µs and (915 ± 91) µs. At hydrogen dilution R = 1 series *LP* sample after HPT shows a negative trend, a comparable drop is obvious for most samples at R = 1.5. The reason for that could be low minority carrier bulk lifetimes of single c-Si wafers. As before, the overall positive changes in the material properties after APT are confirmed here by an increased effective lifetime of minority carriers. In summary, the passivation quality of argon and hydrogen post-deposition treated i-a-Si:H samples are changing and similarly, the microstructure and strength factors are changing. Thus, the more compact the material the better the overall passivation quality. As stated by several research groups an abrupt a-Si:H/c-Si interface is favorable over a less abrupt interface [18,25,37]. Although we could not clarify this fact here the results suggest that after argon plasma treatment the interface between the c-Si(n) substrate and the i-a-Si:H layer becomes more abrupt than after HPT. This could be explained by the lower *ms* values, higher strength and significantly increased minority carrier lifetime after APT.

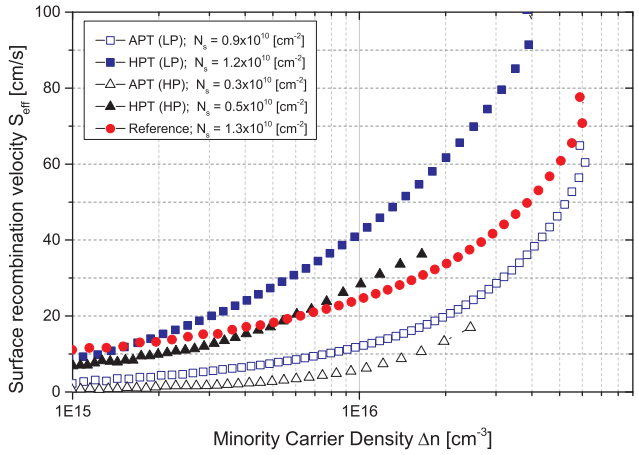

Fig. 5. Injection level dependent S_{eff} for two samples from each series *LP* and series *HP* after APT and HPT and a reference sample without plasma treatment.

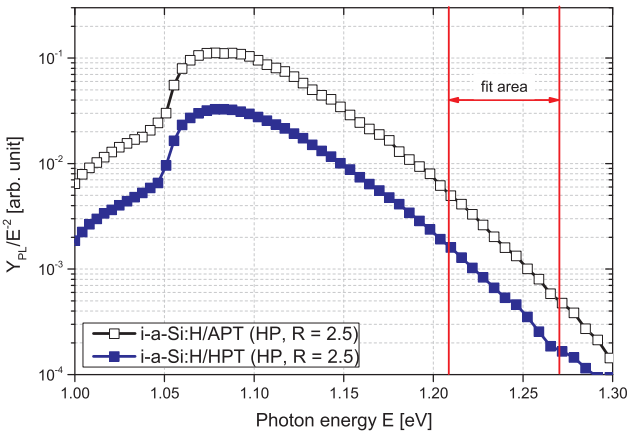

Fig. 6. Photoluminescence spectra of i-a-Si:H (*HR* series, R = 2.5) passivated textured c-Si wafers. Within the marked *fit area* the Temperature and the quasi-Fermi level splitting were analyzed.

From the two sets of samples, we have taken i-a-Si:H samples deposited at R = 2.5 as they are most useful in SHJ-SC's due to their high effective lifetime values. We studied the recombination at the i-a-Si:H/c-Si heterointerface as suggested by Olibet et al. taking the amphoteric nature of silicon dangling bonds into account [25]. The effective surface recombination velocity (S_{eff}) and the interface dangling bond density (N_s) can be calculated according to Eq. (1) by evaluating the measured effective lifetime (τ_{eff}) depending on the minority carrier density (Δ n). Results determined in this way are depicted in Fig. 5. N_s is lower after APT compared to HPT for the same i-a-Si:H layer but different post-deposition plasma treatment. In fact, the i-a-Si:H layer deposited at 19 mW/cm^2 shows a calculated N_s value of $0.9 \cdot 10^{10}$ cm^{-2} after APT, the same layer after HPT exposure has a higher N_s value of $1.2 \cdot 10^{10}$ cm^{-2}. When the i-a-Si:H layers are grown at deposition power densities of 38 mW/cm^2, a post-deposition APT reduces N_s to $0.3 \cdot 10^{10}$ cm^{-2}. After HPT the interface dangling bond density is again higher ($0.5 \cdot 10^{10}$ cm^{-2}). The untreated i-a-Si:H reference sample (red dots) shows the highest surface recombination velocity at minority carrier densities of $1 \cdot 10^{-15}$ cm^{-3} resulting in a N_s value of $2.3 \cdot 10^{10}$ cm^{-2}.

The interface dangling bond density of HPT samples is obviously higher than of samples treated in argon plasma. As described above, a trend towards lower microstructures and the formation of isolated monohybrid bonds after APT is favored. These findings are highly interesting as an unique consistency between several results and especially the formation of interface silicon–hydrogen bonds is observed.

In order to demonstrate the i-a-Si:H passivation effect on the surface of (111) n-doped c-Si wafers, photoluminescence (PL) and surface photovoltage (SPV) measurements were conducted. With these, it is possible to determine the relative quasi-Fermi level (QFL) splitting μ and to compare the results with effective lifetime measurements. Here, we only investigate samples with the highest effective lifetime (R = 2.5, series *HP*).

In Fig. 6 the measured photoluminescence spectra are presented. In order to specify the temperature (T) and the QFL splitting (μ), the red-labeled region, $1.21 \leqq E \leqq 1.27$ eV, is selected and analyzed according to Eq. (2). From the linear fit, the average temperature was determined to be 296.6 K. Moreover, several measurements on the same spot were conducted to observe whether the relatively high laser intensity has an influence on the measurements. According to the measured PL spectra, the individual measurements clearly show same results. The robustness of the outcomes suggests the high validity of the results. In addition, both samples were illuminated by the same laser intensity which leads to the fact that a relative distinction is possible. Therefore, we introduce the parameter $\Delta\mu$ to determine the absolute difference in μ between argon and hydrogen post-deposition treated samples with the result that the absolute difference of QFL splitting after APT is higher by $\Delta\mu = 29$ meV compared to hydrogen treated samples. From this result we can deduce that due to the decreased non-radiative recombination, the QFL splitting is higher and therefore the V_{oc} in finished SHJ solar cells could be higher by approximately 29 mV. That is mainly due to a better surface passivation and confirms our above-mentioned relation of effective lifetime measurements, interface dangling bond density states and more compact i-a-Si:H material properties after APT compared to HPT.

To finalize our single layer characterization results we conducted SPV measurements to correlate the gained results with PL and effective lifetime measurements. The difference of the surface photovoltage in dark and illuminated conditions (Δ SPV) is 250 mV and 220 mV after APT or HPT, respectively. Since the SPV measurement provides electronic information from both the bulk and the surface of c-Si(n) substrates we can conclude that a higher Δ SPV can be attributed to a better interface passivation since we used the same c-Si(n) substrate with comparable or similar bulk properties.

In Table 2 the results of our series *HP* samples deposited at the highest hydrogen dilution (R = 2.5) are summarized as this i-a-Si:H layer will be used as the passivation layer for SHJ solar cell fabrication. An increase in material compactness and in strength as well as a decrease in *ms* is distinct when applying APT instead of HPT. Moreover, similar trends are observed for both series and all hydrogen dilution ratios ($0 \leqq R \leqq 2.5$). Effective lifetime, PL and SPV measurements were conducted to understand the effect of surface passivation changes after post-deposition argon or hydrogen plasma treatment. The corresponding effective lifetime measurements show a correlation between the Δ SPV values as well as to the splitting of the quasi-Fermi level μ. Although neither our PL measurements nor the SPV measurements indicate absolute values the stated conclusions from effective lifetime, spectroscopic ellipsometry and infrared measurements are still supported. A significant difference between argon and hydrogen plasma treatment methods is also shown by the i-a-Si:H/c-Si interface defect

Table 2
Summary of i-a-Si:H layers, deposited at R = 2.5 and RF − P = 38 mW/cm^2, after APT or HPT.

	APT	HPT
strength [–]	8.21 ± 0.21	7.42 ± 0.19
ms [–]	0.35 ± 0.01	0.40 ± 0.02
$\Delta\mu$ [meV]	29	–
Δ SPV [mV]	250	220
τ_{eff} [μs]	915 ± 92	483 ± 48
N_s [10^{10} cm^{-2}]	0.3	0.5

Table 3
SHJ solar cells parameters after APT, HPT, and no PT. To calculate the pseudo solar conversion efficiency (pη) the short current density (j_{sc}) was set to 35 mA/cm^2 according to external quantum efficiency measurements.

	pV_{oc} [mV]	pFF [%]	pη [%]
APT	708.0 ± 11.6	79.3 ± 1.0	19.6 ± 0.4
HPT	689.6 ± 6.8	80.5 ± 1.0	19.3 ± 0.3
No PT	659.7 ± 36.8	75.1 ± 10.6	17.4 ± 3.0

state density N_s.

3.3. SHJ solar cell results

After introducing argon plasma treatment on thin i-a-Si:H layers and demonstrating beneficial effects especially for the minority carrier lifetime after APT, we implemented interface passivation steps in SHJ solar cells. In particular, we used 5–6 nm thick i-a-Si:H layers deposited at 38 mW/cm^2 and a hydrogen dilution of R = 2.5. The Suns − V_{oc} results are summarized in Table 3, the standard deviation is obtained from individual measurements on 2 × 2 cm^2 lab sized SHJ solar cells.

The first two lines in Table 3 compare post-deposition argon and hydrogen treated samples, respectively. To demonstrate the positive effect of both post-deposition plasma treatment methods we introduce reference SHJ solar cells without any plasma treatment (no PT). The pV_{oc} increases significantly on average with APT compared to HPT samples from (689.6 ± 6.8) mV to (708.0 ± 11.6) mV. Without plasma treatment after i-a-Si:H layer deposition the pV_{oc} is even lower (659.7 mV). APT and HPT samples have a similar pFF with (79.3 ± 1.0)% and (80.5 ± 1.0)%, respectively. The same sample without plasma treatment shows a little lower pFF, (75.1 ± 10.6)%. Based on this results it can be also seen that with APT and HPT the variance of pV_{oc} and pFF is lower and therefore the obtained values are more uniform across the sample. Most likely the differences due to thickness inhomogeneities or layer quality are reduced by the more compact structure and by reduced interface dangling bond density states with post-deposition plasma treatment. If considering the short current density (j_{sc}) to be 35 mA/cm^2, obtained by external quantum efficiency measurements, the pseudo solar conversion efficiencies in SHJ solar cells after APT, HPT and without PT are (19.6 ± 0.3)%, (19.3 ± 0.3)% and (17.4 ± 3.0)%, respectively. Considering only the best single cell results we have achieved even higher pV_{oc} values of 720.5 mV after APT. By comparison this pV_{oc} values of APT samples with HPT (pV_{oc} = 703.4 mV) and no PT (pV_{oc} = 682.5 mV) samples demonstrates again the outstanding performance and the positive influence of an optimized interface post-deposition argon plasma treatment step.

The most important conclusion which can be drawn from the pV_{oc} measurements is the clear relationship between the variables determined in the section before. As it was shown from PL measurements $\Delta\mu$ after APT had an absolute difference to HPT samples by 29 meV which directly reflected in our SHJ solar cells, the pV_{oc} difference here is almost 20 mV in average. Obviously the difference between $\Delta\mu$ and pV_{oc} can be deduced from the fact that the n- and p-doped layers and the electrodes have an influence to the effective QFL splitting, the electrical bandgap is not equal to the optical bandgap. In addition, the pV_{oc} were extracted from effective minority carrier lifetime measurements. The resulting pV_{oc} values after APT, HPT and no PT for the same i-a-Si:H layer as used in this SHJ solar cells structure are 718 mV, 692 mV, and 679 mV, respectively. Thus, the demonstrated pV_{oc} and their absolute differences are confirmed by PL and effective lifetime measurements.

It can be summarized that ATP has significant advantages over HPT and no PT, when applying as i-a-Si:H post-deposition plasma treatment step. The advantages are mostly in structural changes of the underlying i-a-Si:H layer, improved passivation of dangling bonds at the a-Si:H/c-Si interface and thus a more effective minority carrier lifetime and quasi-Fermi level splitting.

4. Conclusion

We have presented an extensive study of post-deposition argon and hydrogen plasma treatment on the surface of thin i-a-Si:H layers and their influence in SHJ solar cells. Two sets of samples were presented to demonstrate the change of void structure and passivation quality after APT and HPT in comparison for different hydrogen dilutions and deposition power densities during i-a-Si:H layer growth. The experiments showed that depending on the hydrogen dilution and deposition power densities the microstructure, strength and effective minority carrier lifetime of the i-a-Si:H layer changed. The influence of APT and HPT to the i-a-Si:H layer itself and to the a-Si:H/c-Si interface are consistent and show that the interface most likely becomes more abrupt and better passivated due to reduced hydrogen concentration at the heterointerface. This suggests that APT neutralizes material stress at the surface and leads to a transfer of hydrogen from a higher silicon-hybrid to a monohybrid state at the interface. Thus, the silicon network becomes more compact and therefore the passivation quality improves after APT. This was shown with the help of effective lifetime, photoluminescence and surface photovoltage measurements. In addition, SHJ solar cells were fabricated to demonstrate the difference between APT and HPT on the open-circuit voltage and the influence on the solar conversion efficiency. As a result, a significant increase in the open-circuit voltage was observed after APT. Overall, the study presented here provides a coherent interpretation of the various results with important discoveries to complete the understanding of interfaces in SHJ solar cells.

Acknowledgment

The authors thank Ivan Shutsko, Martin Kellermann, and Maike Ahrlich for support with HF dips. Financial support from the Estonian Ministry of Higher Education and Research (Project IUT19-28), ERA.Net RUS Plus (reference number ETAG15028, FLEXAPP) and the German Federal Ministry of Economics and Technology (BMWi, reference number 0325825H, HERA) are gratefully acknowledged.

References

[1] A.G. Aberle, S. Glunz, W. Warta, Impact of illumination level and oxide parameters on Shockley–Read–Hall recombination at the Si-SiO2 interface, J. Appl. Phys. 71 (9) (1992) 4422–4431.
[2] O. Schultz, S.W. Glunz, G.P. Willeke, Short communication: accelerated publication: Multicrystalline silicon solar cells exceeding 20% efficiency, Prog. Photovolt.: Res. Appl. 12 (7) (2004) 553–558.
[3] K. Yasutake, Z. Chen, S.K. Pang, A. Rohatgi, Modeling and characterization of interface state parameters and surface recombination velocity at plasma enhanced chemical vapor deposited SiO_2 − Si interface, J. Appl. Phys. 75 (4) (1994) 2048–2054.
[4] T. Lauinger, J. Schmidt, A.G. Aberle, R. Hezel, Record low surface recombination velocities on 1 $\omega\cdot$ cmp − silicon using remote plasma silicon nitride passivation, Appl. Phys. Lett. 68 (9) (1996) 1232–1234.
[5] H. Mäckel, R. Lüdemann, Detailed study of the composition of hydrogenated SiN_x layers for high-quality silicon surface passivation, J. Appl. Phys. 92 (5) (2002) 2602–2609.
[6] A.G. Aberle, Overview on SiN surface passivation of crystalline silicon solar cells, Sol. Energy Mater. Sol. Cells 65 (14) (2001) 239–248 (PVSEC 11 Part I).
[7] S. Janz, S. Riepe, M. Hofmann, S. Reber, S. Glunz, Phosphorus-doped SiC as an excellent p-type Si surface passivation layer, Appl. Phys. Lett. 88, 13.
[8] G. Dingemans, W.M.M. Kessels, Status and prospects of Al_2O_3-based surface passivation schemes for silicon solar cells, J. Vac. Sci. Technol. A, 30, 4.
[9] B. Hoex, S.B.S. Heil, E. Langereis, M.C.M. van de Sanden, W.M.M. Kessels, Ultralow surface recombination of c-si substrates passivated by plasma-assisted atomic layer deposited Al_2O_3, Appl. Phys. Lett. 89, 4.
[10] S. De Wolf, A. Descoeudres, Z.C. Holman, et al., High-efficiency silicon heterojunction solar cells: a review, Green 2 (1) (2012) 7–24.
[11] J.I. Pankove, M.L. Tarng, Amorphous silicon as a passivant for crystalline silicon, Appl. Phys. Lett. 34 (2) (1979) 156–157.
[12] K. Masuko, M. Shigematsu, T. Hashiguchi, D. Fujishima, M. Kai, N. Yoshimura, T. Yamaguchi, Y. Ichihashi, T. Mishima, N. Matsubara, T. Yamanishi, T. Takahama, M. Taguchi, E. Maruyama, S. Okamoto, Achievement of more than 25%; conversion efficiency with crystalline silicon heterojunction solar cell, IEEE J. Photovolt. 4 (6) (2014) 1433–1435.
[13] M. Mews, T.F. Schulze, N. Mingirulli, L. Korte, Hydrogen plasma treatments for passivation of amorphous-crystalline silicon-heterojunctions on surfaces promoting

epitaxy, Appl. Phys. Lett. 102, 12.
[14] L. Zhang, W. Guo, W. Liu, J. Bao, J. Liu, J. Shi, F. Meng, Z. Liu, Investigation of positive roles of hydrogen plasma treatment for interface passivation based on silicon heterojunction solar cells, J. Phys. D: Appl. Phys. 49 (16) (2016) 165305.
[15] A. Descoeudres, L. Barraud, S. De Wolf, B. Strahm, D. Lachenal, C. Guérin, Z.C. Holman, F. Zicarelli, B. Demaurex, J. Seif, J. Holovsky, C. Ballif, Improved amorphous/crystalline silicon interface passivation by hydrogen plasma treatment, Appl. Phys. Lett. 99, 12.
[16] A.H.M. Smets, W.M.M. Kessels, M.C.M. van de Sanden, The effect of ion-surface and ion-bulk interactions during hydrogenated amorphous silicon deposition, J. Appl. Phys. 102, 7.
[17] U.K. Das, M.Z. Burrows, M. Lu, S. Bowden, R.W. Birkmire, Surface passivation and heterojunction cells on Si (100) and (111) wafers using dc and rf plasma deposited Si: H thin films, Appl. Phys. Lett. 92, 6.
[18] J. Damon-Lacoste, P. Roca i Cabarrocas, Toward a better physical understanding of a − Si: H/c − Si heterojunction solar cells, J. Appl. Phys. 105 (6) (2009) 63712.
[19] A. Neumüller, O. Sergeev, M. Vehse, C. Agert, Argon plasma treatment at the i-/p-interface in silicon thin-film solar cells and its influence on the light induced degradation, Energy Procedia 84 (2015) 242–250.
[20] W. Beyer, D. Lennartz, P. Prunici, H. Stiebig, Annealing effects of microstructure in thin-film silicon solar cell materials measured by effusion of implanted rare gas atoms, MRS Proc. 1321.
[21] S.K. O'Leary, S.R. Johnson, P.K. Lim, The relationship between the distribution of electronic states and the optical absorption spectrum of an amorphous semiconductor: an empirical analysis, J. Appl. Phys. 82 (7) (1997) 3334–3340.
[22] G. Jellison, Spectroscopic ellipsometry data analysis: measured versus calculated quantities, Thin Solid Films 313314 (1998) 33–39.
[23] M. Cardona, Vibrational spectra of hydrogen in silicon and germanium, Phys. Status Solidi (B) 118 (2) (1983) 463–481.
[24] A.H.M. Smets, M.C.M. van de Sanden, Relation of the SiH stretching frequency to the nanostructural SiH bulk environment, Phys. Rev. B 76 (2007) 073202.
[25] S. Olibet, E. Vallat-Sauvain, C. Ballif, Model for a-Si: H/c-Si interface recombination based on the amphoteric nature of silicon dangling bonds, Phys. Rev. B 76 (2007) 035326.
[26] B. Bahardoust, A. Chutinan, K. Leong, A.B. Gougam, D. Yeghikyan, T. Kosteski, N.P. Kherani, S. Zukotynski, Passivation study of the amorphous? Crystalline silicon interface formed using dc saddle-field glow discharge, Phys. Status Solidi A 207 (3) (2010) 539–543.
[27] M. Meaudre, R. Meaudre, Determination of the capture cross sections of electrons in undoped hydrogenated amorphous silicon from the photoconductivity of and space-charge relaxation in $n^+i - n^+$ structures; the role of light exposure and annealing, J. Phys.: Condens. Matter 13 (24) (2001) 5663.
[28] D. Abou-Ras, T. Kirchartz, U. Rau, Advanced Characterization Techniques for Thin Film Solar Cells, John Wiley & Sons, New York, 2011.
[29] N. Revathi, S. Bereznev, M. Loorits, J. Raudoja, J. Lehner, J. Gurevits, R. Traksmaa, V. Mikli, E. Mellikov, O. Volobujeva, Annealing effect for SnS thin films prepared by high-vacuum evaporation, J. Vac. Sci. Technol. A, 32, 6.
[30] T. Shimizu, K. Nakazawa, M. Kumeda, S. Ueda, Incorporation scheme of H reducing defects in a − Si studied by NMR and ESR, Physica B + C 117 (1983) 926–928.
[31] A.H. Mahan, P. Raboisson, R. Tsu, Influence of microstructure on the photoconductivity of glow discharge deposited amorphous SiC: H and amorphous SiGe: H alloys, Appl. Phys. Lett. 50 (6) (1987) 335–337.
[32] A.H. Mahan, P. Menna, R. Tsu, Influence of microstructure on the urbach edge of amorphous SiC: H and amorphous SiGe: H alloys, Appl. Phys. Lett. 51 (15) (1987) 1167–1169.
[33] Y. Toyoshima, K. Kumata, U. Itoh, K. Arai, A. Matsuda, N. Washida, G. Inoue, K. Katsuumi, Ar($^3P_2$) induced chemical vapor deposition of hydrogenated amorphous silicon, Appl. Phys. Lett. 46 (6) (1985) 584–586.
[34] M.Z. Burrows, U.K. Das, R.L. Opila, S. De Wolf, R.W. Birkmire, Role of hydrogen bonding environment in a-Si: H films for c-Si surface passivation, J. Vac. Sci. Technol. A 26 (4) (2008) 683–687.
[35] H. Fujiwara, Y. Toyoshima, M. Kondo, A. Matsuda, Interface-layer formation mechanism in a − Si: H thin-film growth studied by real-time spectroscopic ellipsometry and infrared spectroscopy, Phys. Rev. B 60 (1999) 13598–13604.
[36] A. Neumüller, O. Sergeev, M. Vehse, C. Agert, Structural characterization of the interface structure of amorphous silicon thin films after post-deposition argon or hydrogen plasma treatment, Appl. Surf. Sci. 403 (Supplement C) (2017) S200–S205.
[37] S. De Wolf, M. Kondo, Abruptness of a − Si: H/c − Si interface revealed by carrier lifetime measurements, Appl. Phys. Lett. 90, 4.

Dr. Martin Vehse is head of the department Urban and Residential Technologies at the DLR Institute of Networked Energy Systems. He studied physics at the University of Bremen, finished his Ph.D. study with the doctoral level in 2001. Afterwards, he spent a post-doctoral period at the University of California, Santa Barbara at the Institute for Polymers and Organic Solids, working in the field of conducting polymers. In 2004, he started his professional carrier as project manager on OLED technology at the company Novaled GmbH, and joined the photovoltaics activities at the research institute NEXT ENERGY in August 2010. Since 2017 he is working at the German Aerospace Center.

Prof. Dr. Carsten Agert studied physics at the Universities of Marburg and Canterbury. After he earned his doctorate at the Fraunhofer Institute for Solar Energy Systems (ISE) in Freiburg, he conducted research and worked while in Oxford and Pretoria. In 2002, he returned to the Fraunhofer ISE, where he coordinated strategic planning for the institute's areas of business and later directed a fuel cell research group. Since 2008, He has been Professor for Energy Technology at the University of Oldenburg. He is Head of the EWE Research Centre NEXT ENERGY, which was integrated in the German Aerospace Center, as DLR Institute of Networked Energy Systems, in 2017.

Jose Fabio Lopez Salas received his B.Sc. in Physics from the Karlsruhe Institute of Technology in 2012 and his M.Sc. in Physics from the University of Oldenburg in 2014. He is currently a Ph.D. candidate at the Laboratory of Chalcogenide Photovoltaics in the department of Energy and Semiconductor Research at the University of Oldenburg, Germany. His research focuses on the device simulation and simulation of charge carrier lifetimes in CIGS thin film solar cells.

Oleg Sergeev owned his Ph.D. in Material Science in the field of light-emitting sol-gel nanostructures in 2001. His postdoctoral research at the University of Wuppertal, Germany was devoted to the development and application of novel characterization techniques like near-field cathodoluminescence and hybrid SNOM/SEM microscopy. Since 2009 he is developing solar cells at EWE Research Centre for Energy Technology NEXT ENERGY (since 2017 DLR Institute of Networked Energy Systems) in Oldenburg.

Stephan J. Heise received his diploma in Physics from the University of Cologne in 2005 and his Ph.D. from the University of Oldenburg in 2009. He currently works as a postdoctoral researcher at the Laboratory of Chalcogenide Photovoltaics in the department of Energy and Semiconductor Research at the University of Oldenburg, Germany. His research is focussed on the characterization of charge carrier dynamics in chalcogenide-based thin films and solar cell devices by optoelectronic methods and device simulations.

Dr. Olga Volobujeva is currently Senior Researcher in Department of Materials and Environmental Technology at the Tallinn University of Technology. She obtained her Ph.D. in Chemical and Material Science from TUT in 2008. Her research focuses on fabrication and characterization of chalcogenide-based thin film solar cells.

Sergei Bereznev received his Diploma Engineer degree in 1993 in semiconductors technology from Tallinn University of Technology (TUT), Estonia, M.S. degree in 2000 in chemical technology from TUT, and Ph.D. degree in 2003 in chemical and material science from TUT. He worked as a researcher and senior researcher at the Department of Materials Science, TUT from 2000 to 2016. He is currently an associate professor in the Department of Materials and Environmental Technology at TUT. His current research interests include the development of novel functional layers and hybrid structures for optoelectronics, nanoscale coatings, and growth studies of nanostructures.

Alex Neumüller studied physics at the University of Bonn and later in Oldenburg, Germany. After receiving his M.Sc. in Physics at the EWE Research Centre for Energy Technology NEXT ENERGY in 2013, he started a Ph.D. in the photovoltaics division at the same institute. In the framework of his Ph.D. studies, which he has successfully finished in 2017, he investigated the heterointerfaces in crystalline silicon based solar cells.